Supporting Information for "The Hunga Tonga-Hunga Ha'apai Hydration of the Stratosphere"

L. Millán[1], M. L. Santee[1], A. Lambert[1], N. J. Livesey[1], F. Werner[1], M. J.

Schwartz[1], H. C. Pumphrey[2], G. L. Manney[3,4], Y. Wang[5,1], H. Su[1], L. Wu[1],

W. G. Read[1], and L. Froidevaux[1]

[1]Jet Propulsion Laboratory, California Institute of Technology, Pasadena, California, USA

[2]School of GeoSciences, The University of Edinburgh, Edinburgh, UK

[3]NorthWest Research Associates, Socorro, New Mexico, USA

[4]New Mexico Institute of Mining and Technology, Socorro, New Mexico, USA

[5]Division of Geological and Planetary Sciences, California Institute of Technology, Pasadena, CA, USA

Contents of this file

1. Figures S1, S2, and S3

Introduction

The main document describes volcanic stratospheric enhancements in H_2O, SO_2, and HCl mixing ratios as measured by the Aura Microwave Limb Sounder (MLS) (Waters et al., 2006; Livesey et al., 2020) following the 15 January 2022 Hunga Tonga-Hunga Ha'apai (HT-HH) eruption. In particular, the main document describes the unprecedented H_2O injection. Supporting information contains additional figures supplementing the discussion in the main text.

————

May 4, 2022, 2:52pm

Figure S1 shows examples of the anomalous mixing ratios encountered in the HT-HH plume for most of the trace gases retrieved by MLS. Anomalous mixing ratios are identified as data points with values greater (lower) than 7 standard deviations above (below) the climatological January-February-March (JFM) 2005–2021 average. As mentioned in the main document, anomalous values in products other than H_2O, SO_2, and HCl in the HT-HH plume are believed to be artifacts arising from SO_2 spectral interference. Note that many of these anomalous values are negative. Many MLS measurements have poor signal to noise ratio for individual profiles; for these species, radiance noise, combined with negative "lobes" in averaging kernels (Livesey et al., 2020), can lead to the retrieval of negative mixing ratios.

Figure S2a shows the longitude of $10\,hPa$ H_2O outliers with mixing ratios exceeding $11\,ppmv$; the HT-HH plume circles the globe four times at this level in the first two and a half months after the eruption. Figure S2b shows a linear fit through the "unwrapped" longitudes of these outliers with respect to time, showing that the plume was advected by consistent easterly flow at this level throughout the study period. Figure S2c compares the slopes of similar fits to outlier locations at stratospheric retrieval levels from $83\,hPa$ to $1\,hPa$ (red line) with the level averages of degrees of longitude per day at outlier locations derived from GEOS-5.12.4 winds (black line). Thresholds defining "outliers" at a given level were selected to highlight each level's primary plume. A small number of outliers that were not located within the primary HT-HH plume have been removed at some levels. Analysis winds are interpolated to MLS measurement locations as described by Manney et al. (2007).

May 4, 2022, 2:52pm

Figure S3a shows the zonal mean H_2O measured by MLS in February 2022. Figure S3b shows the effective radiative forcing response due to the excess H_2O, calculated based on climate simulations from the National Center for Atmospheric Research (NCAR) Community Earth System Model (CESM) version 1.2.1. We use the downwelling long-wave radiation flux output at the tropopause level to diagnose stratospheric H_2O radiative forcing (Forster et al., 2001; Wang et al., 2017). The effective radiative forcing includes both the instantaneous forcing and atmospheric and land adjustments (Smith et al., 2020), and it is widely used in the recent IPCC Assessment Reports (e.g., Myhre et al., 2013). A pair of 10-year CESM simulations were conducted with present-day radiative forcing from other agents, such as greenhouse gases, aerosols, etc. Sea surface temperature and sea ice were prescribed using the present-day climatology. Both runs were nudged to time-invariant zonal mean stratospheric H_2O fields, with the control run nudged to an MLS-derived (2005–2013) climatology, and the sensitivity run nudged to the same climatology augmented by the 2022 February anomaly. The average differences between the runs over the last 9 years of the simulations are used for the forcing calculation (the first year was used for model spin-up).

References

Forster, P. M., Ponater, M., & Zhong, W.-Y. (2001). Testing broadband radiation schemes for their ability to calculate the radiative forcing and temperature response to stratospheric water vapour and ozone changes. *Meteorologische Zeitschrift*, *10*(5), 387–393. Retrieved from `https://doi.org/10.1127/0941-2948/2001/0010-0387` doi: 10.1127/0941-2948/2001/0010-0387

Livesey, N. J., Read, W., Wagner, L., P. A. Froidevaux, Lambert, A., Manney, G. L.,

Millán Valle, L., ... R., L. R. (2020). *Version 4.2x Level 2 and 3 data quality and description document* (Tech. Rep. No. JPL D-33509 Rev. E). Jet Propulsion Laboratory. Retrieved from `http://mls.jpl.nasa.gov`

Manney, G. L., Daffer, W. H., Zawodny, J. M., Bernath, P. F., Hoppel, K. W., Walker, K. A., ... Waters, J. W. (2007). Solar occultation satellite data and derived meteorological products: Sampling issues and comparisons with Aura Microwave Limb Sounder. *Journal of Geophysical Research*, *112*(D24). Retrieved from `https://doi.org/10.1029/2007jd008709` doi: 10.1029/2007jd008709

Myhre, G., Shindell, D., Bréon, F.-M., Collins, W., Fuglestvedt, J., Huang, J., ... Zhang, H. (2013). Anthropogenic and natural radiative forcing. In T. F. Stocker et al. (Eds.), *Climate Change 2013: The Physical Science Basis. Contribution of Working Group I to the Fifth Assessment Report of the Intergovernmental Panel on Climate Change* (pp. 659–740). Cambridge, UK: Cambridge University Press. doi: 10.1017/CBO9781107415324.018

Smith, C. J., Kramer, R. J., Myhre, G., Alterskjær, K., Collins, W., Sima, A., ... Forster, P. M. (2020). Effective radiative forcing and adjustments in CMIP6 models. *Atmospheric Chemistry and Physics*, *20*(16), 9591–9618. Retrieved from `https://doi.org/10.5194/acp-20-9591-2020` doi: 10.5194/acp-20-9591-2020

Wang, Y., Su, H., Jiang, J. H., Livesey, N. J., Santee, M. L., Froidevaux, L., ... Anderson, J. (2017). The linkage between stratospheric water vapor and surface temperature in an observation-constrained coupled general circulation model. *Climate Dynamics*, *48*(7-8), 2671–2683. Retrieved from `https://doi.org/10.1007/s00382-016-3231-3` doi: 10.1007/s00382-016-3231-3

Waters, J., Froidevaux, L., Harwood, R., Jarnot, R., Pickett, H., Read, W., ... Walch, M. (2006). The Earth observing system Microwave Limb Sounder (EOS MLS) on the Aura Satellite. *IEEE Transactions on Geoscience and Remote Sensing*, *44*(5), 1075–1092. Retrieved from `https://doi.org/10.1109/tgrs.2006.873771` doi: 10.1109/tgrs.2006.873771
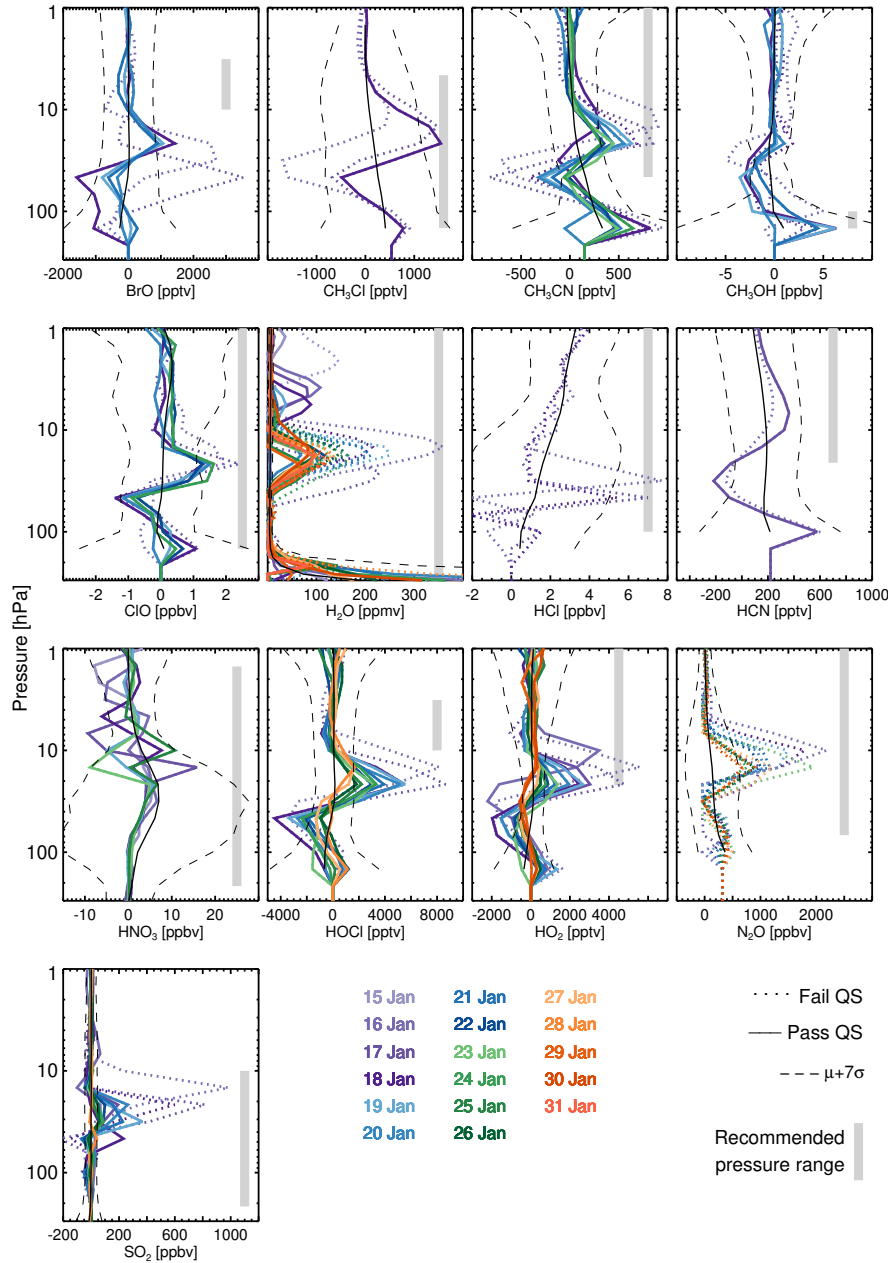
Figure S1. Anomalous profiles after the HT-HH eruption for several MLS trace gases. For clarity, only the profile with the maximum enhancement or deficit is shown for each day; individual days are represented by colored lines (see legend). Dotted lines indicate that the profile did not pass the quality screening (QS) criteria; solid lines indicate that it did. The climatological January-February-March 2005–2021 mean is shown by a solid black line. The black dashed lines show values 7 standard deviations above and below the mean for each trace gas; these lines are used to identify enhancements or deficits. The gray vertical bars mark the recommended pressure range for typical conditions as described in the MLS data quality document (Livesey et al., 2020).
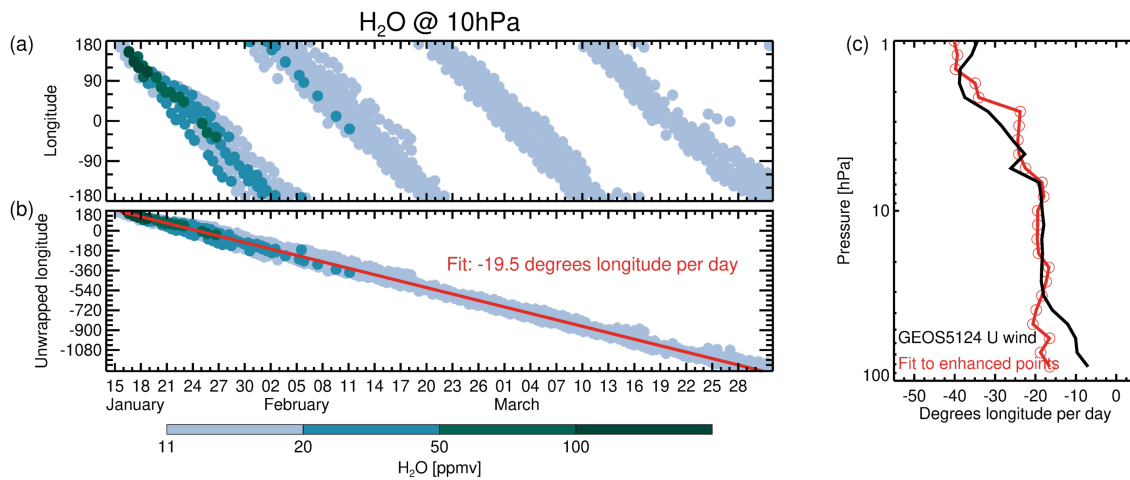
May 4, 2022, 2:52pm

Figure S2. (a) Longitudes of enhanced $10\,\mathrm{hPa}$ H_2O (a mixing ratio threshold of $> 11\,\mathrm{ppmv}$ is used to define outliers at this level) as a function of time. Colors represent different H_2O abundances. (b) The enhanced H_2O values shown in (a) but using "unwrapped" longitude. The red line is a linear fit through these points. (c) Slopes from linear fits through enhanced H_2O values at different pressure levels (red line), as well as the averaged degrees-longitude-per-day at each level derived from GEOS-5.12.4 zonal winds interpolated to the outlier locations.
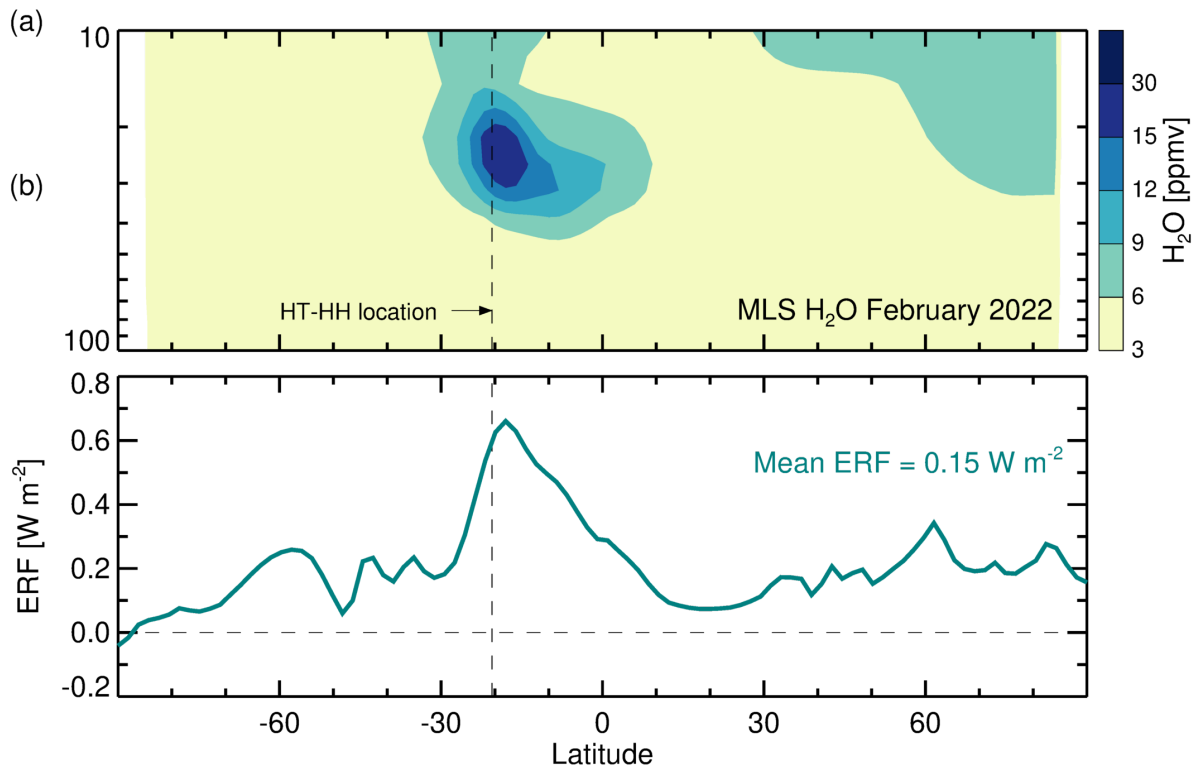
May 4, 2022, 2:52pm

Figure S3. (a) February 2022 MLS zonal mean H_2O measurements, with no quality screening applied. (b) Effective radiative forcing (ERF) at the tropopause due to the February 2022 MLS H_2O anomaly, based on 9 years of model simulations.

May 4, 2022, 2:52pm